IEEE Photonics Journal
An IEEE Photonics Society Publication

Open Access

# Microcavity Fiber SERS Probe Coated With Ag Nanoparticles For Detecting Antibiotic in Milk

Volume 13, Number 2, April 2021

Xinghu Fu
Zhenxing Wang
Jiaxuan Li
Shuangyu Ma
Guangwei Fu
Wa Jin
Weihong Bi
Yanhua Dong

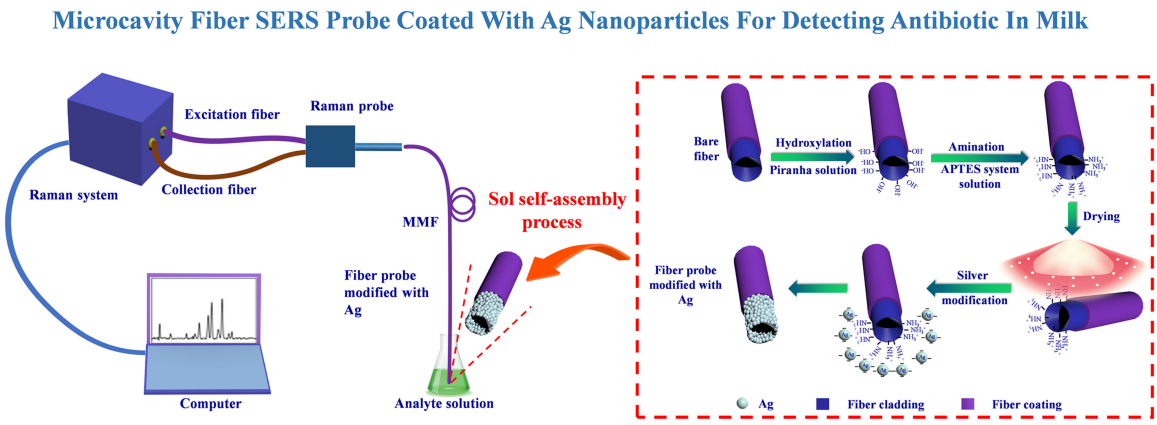


DOI: 10.1109/JPHOT.2021.3064275

# Microcavity Fiber SERS Probe Coated With Ag Nanoparticles For Detecting Antibiotic in Milk

**Xinghu Fu**,[1] **Zhenxing Wang**,[1] **Jiaxuan Li**,[1] **Shuangyu Ma**,[1] **Guangwei Fu**,[1] **Wa Jin**,[1] **Weihong Bi**,[1] **and Yanhua Dong**[2]

[1]School of Information Science and Engineering, The Key Laboratory for Special Fiber and Fiber Sensor of Hebei Province, Yanshan University, Qinhuangdao 066004, China
[2]Key Laboratory of Specialty Fiber Optics and Optical Access Networks, Shanghai University, 200444 Shanghai, China

*DOI:10.1109/JPHOT.2021.3064275*


Manuscript received February 10, 2021; revised March 1, 2021; accepted March 2, 2021. Date of publication March 8, 2021; date of current version March 31, 2021. This work was supported in part by the National Natural Science Foundation of China under Grant 61675176, in part by the Key Basic Research Program of Hebei Province under Grant 17961701D, and in part by the STCSM under Grant SKLSFO2020-02. Corresponding author: Xinghu Fu (e-mail: fuxinghu@ysu.edu.cn)

**Abstract:** In this paper, an Ag nanoparticles (AgNPs) modified multimode fiber (MMF) SERS probe prepared based on sol self-assembly method is proposed and fabricated. Different fiber SERS probes (AgNPs-MMF-x, x is the self-assembly time) are obtained by adjusting the self-assembly time. Using rhodamine 6G (R6G) solution as the probe molecule, the far-end performances of the prepared fiber SERS probe are studied, and the AgNPs-MMF-30 probe with obvious advantages in SERS performance is obtained. The limit of detection (LOD) for R6G is as low as $10^{-9}$ M, demonstrating the high sensitivity of AgNPs-MMF-30 probe. The enhancement factor (EF) of AgNPs-MMF-30 probe to $10^{-7}$ M R6G is about $1.36 \times 10^8$. In addition, the AgNPs-MMF-30 probe has an outstanding reproducibility across the entire area with the maximum value of relative standard deviation (RSD) of less than 10.94%. The AgNPs-MMF-30 probe exhibit a long-term stability regarding Raman enhancement of up to 35 days. Importantly, the high-performance AgNPs-MMF-30 probe is further applied as a highly sensitive SERS platform for the trace detection of antibiotic in milk. The fiber SERS probe has the characteristics of fast, effective, remote real-time detection and so on, so it has great potential application in biochemical sensing and food security.

**Index Terms:** Fiber probe, surface enhanced raman scattering, sol self-assembly, ag nanoparticles, antibiotic.

## 1. Introduction

In recent years, the unreasonable use of antibiotics in animal breeding industry and the content of pollutants in dairy products have aroused people's great attention. Enrofloxacin and Amoxicillin, as common veterinary antibiotics, have obvious effects in the treatment and prevention of animal diseases. However, the abuse of antibiotics has led to the emergence of drug-resistant strains, leading to epidemics [1], [2]. This phenomenon also occurs in milk. In the actual environment, if there are antibiotic residues in milk, long-term consumption will slowly accumulate in the human body, and low concentrations of antibiotic residues may still cause health damage [3]–[5].

Therefore, it has become an important topic in the dairy industry to detect animal antibiotic residues quickly, effectively and in real time.

Currently, the most commonly used detection techniques for enrofloxacin and amoxicillin antibiotics include high-performance liquid chromatography (HPLC) [6], [7], molecularly imprinted polymer method [8], [9], chromatography [10] and liquid mass spectrometry [11], [12]. Although these methods have high accuracy and reliability, they all require complicated pre-processing steps and expensive experimental equipment, long test time, specialized operations and so on. For example, it takes more than 1 hour to detect a single sample by HPLC. Therefore, a simple, rapid and sensitive method for the detection of enrofloxacin and amoxicillin antibiotics in milk is urgently needed. Some researchers use optical detection methods to detect ingredients in milk. Yariv *et al.* [13] introduced a theoretical and practical model for reconstructing the scattering properties of a participating media and presented a novel appearance model for milk parameterized by the lactose and protein contents. Using a novel Gerchberg-Saxton algorithm, they demonstrated the detection of single milk component and isolated its optical behavior, which constitutes the basis for the detection of different components in milk.

Surface enhanced Raman scattering (SERS) spectroscopy has the spectral characteristic of "fingerprint" [14]. It can reflect the molecular structure information, which is an effective method to detect antibiotics. Andreou *et al.* [15] used SERS technology to detect penicillin in milk samples by optimizing the aggregation of silver nanoparticles, and the LOD could reach 10 $\mu$g·mL$^{-1}$. Muhammad *et al.* [16] prepared high-performance periodic nano-silver array substrates by electrochemical deposition using anodized aluminum templates. Using R6G as the probe molecule, they successfully detected $10^{-10}$ M R6G. The substrate was used to detect low concentrations of tetracycline and dicyandiamide in milk, and the LOD were $10^{-9}$ M and $10^{-7}$ M, respectively. However, the disadvantage of these tasks is that they need to rely on expensive large instruments, which are difficult to meet the needs of remote detection and real-time detection.

In recent years, fiber sensors are widely used in environmental, biological and chemical sensing. Kosowska *et al.* [17] prepared a fiber probe by depositing ZnO on the end face of a single-mode fiber and attaching nanocrystalline diamond, and verified its optical properties. In addition, people have combined fiber sensing technology with SERS technology to prepare fiber SERS probe, which can realize large SERS enhancement and good detection reproducibility, simultaneously [18]. The guided mode propagation characteristics of Raman light in the optical fiber can effectively increase the area of light-matter interaction, and the number of excited molecules will increase significantly to increase the intensity of the Raman signal. In addition, the SERS signal collected by fiber probe is the integration of the entire SERS active area, which greatly reduces the uniform distribution requirements of SERS "hot spots" and improves the signal repeatability [19], [20]. It also can prevent contamination of the optical lens of the Raman system when detecting toxic and volatile substances. The fiber SERS probe show advantages such as the capability to identify molecular structure, the high sensitivity of SERS, and remote sensing [21]. Therefore, it can be used in food safety testing [22], pesticide residue chemical analysis [23], biomedical testing [24] and so on. The preparation of fiber SERS probe mainly includes self-assembly method, laser induced chemical deposition method (LICDM), magnetron sputtering method and nanolithography. Yin *et al.* [25] proposed a novel U-shaped fiber SERS probe with high performance based on LICDM, and its sensitivity to R6G was as low as $10^{-8}$ M. Chen *et al.* [26] deposited gold nanoparticles on the surface of a tapered optical fiber through electrostatic self-assembly. The R6G is measured, and the detection limit of R6G aqueous solution reaches $10^{-8}$ M. However, the structure of fiber probe is easy to damage. Elizabeth J Smythe *et al.* [27] proposed a method referred to as "decal transfer" based on electron-beam lithography technology, which could be used to prepare nano-particle cluster structures on the surface of fiber, but the method is complicated to prepare and is not suitable for high throughput probe preparation.

In this paper, we use the self-assembly method to prepare fiber SERS probe by coating AgNPs on the surface of the fiber microcavity structure. Compared with other shapes of fiber probe, the fiber microcavity structure can increase the attachment area of AgNPs and it is not easily damaged, which can effectively increase the area of light-matter interaction. The silver sol is purified

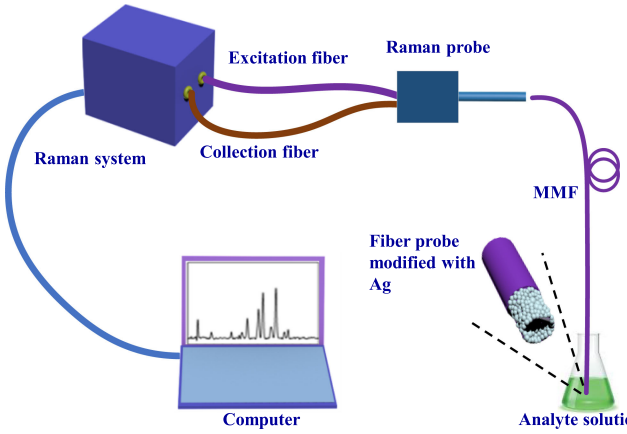


Fig. 1. Experimental device for SERS spectrum detection of microcavity fiber probe.

by high-speed centrifugation, which greatly reduces the self-assembly time. The fiber probe is combined with portable Raman spectrometer to form the SERS system. The whole system is simple and convenient, which can realize remote detection. R6G is used as probe molecule to test the performance of fiber SERS probe. In addition, the detection of antibiotic residues in milk has been successfully achieved. It provides an effective new way for on-site detection of antibiotic residues in milk.

## 2. Experimental

### 2.1. Materials

The graded MMF (core/cladding diameter is 62.5/125 $\mu$m) is fabricated by Yangtze Optical Fiber and Cable Joint Stock Limited Company, China. Hydrofluoric acid (HF: 40%), silver nitrate (99.8%), sodium citrate (99%), ethanol (99.7%), R6G (98%), concentrated sulfuric acid (98%), hydrogen peroxide (30%), 3-aminopropyl triethoxy silane (99%), isopropyl alcohol (99.9%), ammonia (28%), enrofloxacin and amoxicillin are purchased from Aladdin Reagent Limited Company. Deionized water (18.25 M$\Omega$) is used for all solution preparations.

### 2.2. Experimental System Device

In this paper, all Raman spectra are obtained by portable Raman spectrometer with instrument model BWS465-785S, which is equipped with a 785 nm laser. The integration time for each SERS measurement is set to 5s, and the laser power is 240 mW. Fig. 1 is a diagram of the experimental setup. Using wet detection, the fiber probe is put into the solution to be tested. In measurement process, the laser reaches the surface of the microcavity fiber probe modified with AgNPs through the fiber and directly acts on the AgNPs on the inner surface of the core microcavity. The AgNPs adsorbed on the surface of the fiber probe are excited by Raman light and the local surface plasmon resonance effect is generated, so the local electromagnetic field is formed. The SERS signal of the R6G to be measured in the local electromagnetic field will be greatly enhanced. When the R6G molecule is detected at the active end of the fiber probe, the SERS signal generated is transmitted back to the fiber from the end of the fiber probe, and then is collected by the Raman system.

### 2.3. Sample Preparation

Fig. 2 shows the microcavity structure obtained by HF etching the end face of MMF. The total etching time is 10 mins and the etching interval is 1 min.

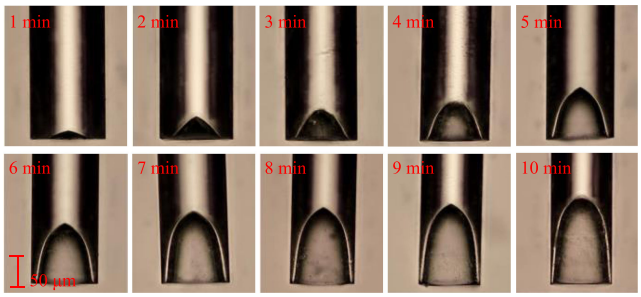


Fig. 2. Fiber microcavity structure with different etching time.

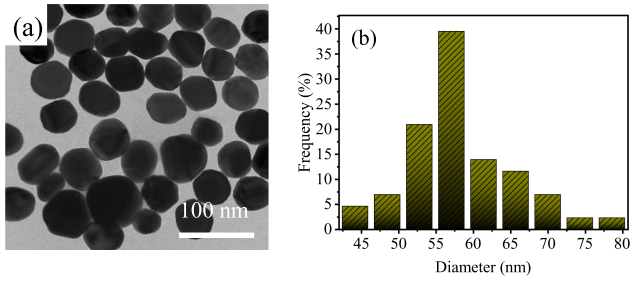


Fig. 3. Experimental results: (a) TEM image of silver sol; (b) size distribution of AgNPs.

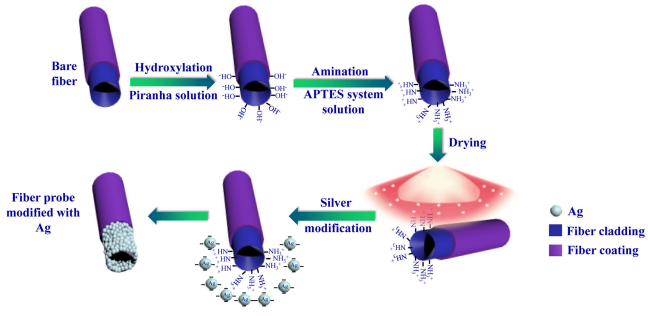


Fig. 4. The experimental process of the self-assembly method of the fiber SERS probe.

The silver sol is prepared by Lee&Meisel chemical method. Fig. 3(a) is the TEM image of the prepared silver sol. The size of AgNPs calculated by Nano Measurer software is between 50 and 65 nm. The average size of AgNPs is about 58 nm.

Fig. 4 concisely illustrates the fabrication process of microcavity structure fiber SERS probe. The silver sol used in the self-assembly process is obtained by centrifugation to reduce the modification time of AgNPs. The centrifugation parameters are 9000 rpm and 15 mins.

The specific modification process is as follows:

Firstly, the prepared microcavity structure of bare fiber is put into piranha solution for 30 mins to make the surface of the fiber hydroxylated (preparation of concentrated sulfuric acid and hydrogen peroxide).

Secondly, the hydroxylated fiber is put into the APTES system solution (preparation of 3-aminopropyl triethoxy silane, isopropyl alcohol and ammonia) for 120 mins to aminate the surface of the fiber. Then the aminated fiber is put into a 100 °C drying oven for 30 mins.

Finally, the dried fiber is placed in the centrifuged nano-silver sol.

By controlling modification time to change the morphology and size of the AgNPs on the surface of the fiber, the fiber SERS probes with different modification time are obtained. The fiber SERS probe is named AgNPs-MMF-x, where x is 10, 20, 30, 40, 50 and 60 mins.

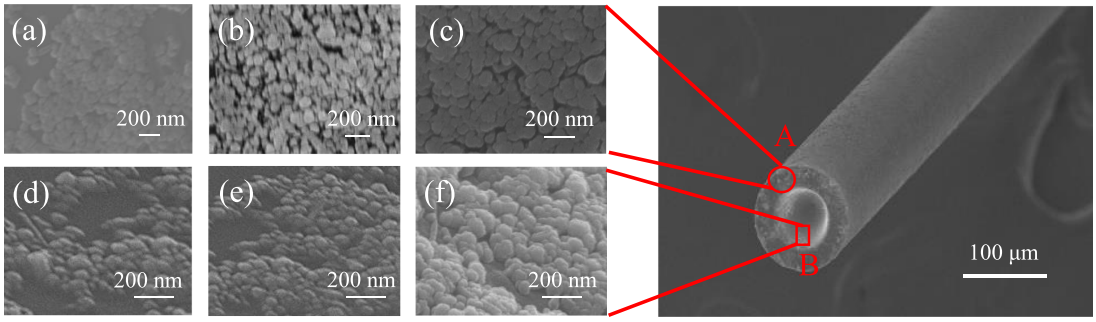


Fig. 5. SEM images of fiber probes with different self-assembly time: A area (a)∼(c) 20, 30, 40 mins; B area (d)∼(f) 20, 30, 40 mins.

Fig. 5 shows the SEM image of the fiber SERS probe prepared by the self-assembly method. Area of A is the end surface area of fiber probe, area of B is the inner surface area of fiber microcavity. Fig. 5(a)∼(c) are the SEM images of A with assembly time of 20, 30 and 40 mins, and Fig. 5(d)∼(f) are the SEM images of B with assembly time of 20, 30 and 40 mins.

It can be seen from Fig. 5 that the growth of AgNPs on the surface of fiber can be controlled by adjusting the self-assembly time. As the self-assembly time increases, the AgNPs in the A area and the B area also increase. The A area basically shows a full single-layer distribution state. Since the B area is inside of the microcavity, it is easy to aggregate the AgNPs when the self-assembly time is the same. When the self-assembly time is 30 mins, a small amount of AgNPs are aggregated in area B, and most of them are still single-layer distribution. When the probe molecule is in the "hot spots" area, the Raman signal will be enhanced. When the self-assembly time exceeds 30 mins, there will be more aggregation of AgNPs.

### 2.4. Detection of Antibiotic in Milk

In this paper, the supernatant is taken for later use after the milk is centrifuged. 50 mg enrofloxacin powder is dissolved in anhydrous ethanol solution and diluted to 50 mL to obtain 1 mg·mL$^{-1}$ enrofloxacin ethanol solution. Then, it is diluted with milk supernatant to obtain enrofloxacin spiked milk samples with different concentrations. It is kept in a refrigerator at 4 °C for three days. It can ensure that the enrofloxacin and the milk supernatant are evenly mixed and can prevent the deterioration of the sample for experimental research. In the same way, different concentrations of amoxicillin labeled milk samples are prepared with deionized water.

## 3. Results and Discussion

### 3.1. Microcavity Structure Selection

This paper uses R6G as a Raman probe molecule, which has been widely applied in SERS detection for its well-established vibrational features. First, the silver sol and R6G with a concentration of $10^{-3}$ M are mixed in equal volume, and the Raman intensity of the mixed solution is measured with bare fibers etched for different time to determine the length of microcavity when the enhancement effect is strongest. As shown in Fig. 6(a), the Raman characteristic peak positions observed at 1184, 1311, 1362, 1510, 1575 and 1651 cm$^{-1}$ are similar to the "fingerprint" peaks of R6G calculated by Schatz *et al.* [28]. The band assignments of R6G are listed in Table 1.

In order to observe the Raman spectrum more clearly, as shown in Fig. 6(b), the Raman position at 1510 cm$^{-1}$ is magnified, it can be seen that when the fiber is etched for 5 mins, the Raman intensity of the mixed solution is the strongest. At this time, the length of microcavity is 80 $\mu$m approximately. Therefore, in the next self-assembly method, the fiber microcavity structure with an etching time of 5 mins is used to modify AgNPS.

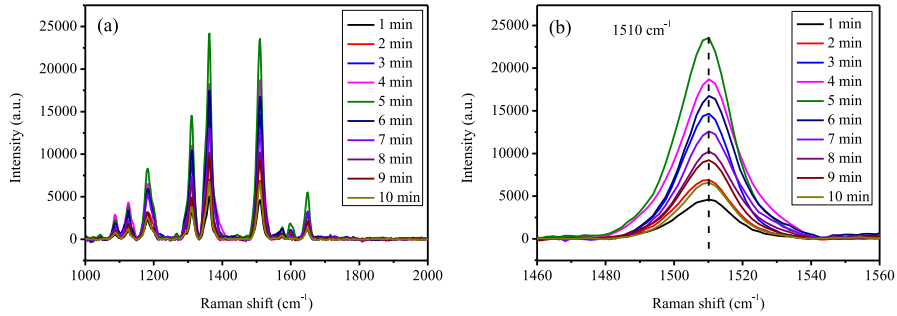


Fig. 6. Experimental results: (a) Raman spectroscopy of mixed solution detected by fiber with different etching time; (b) Raman characteristic peak intensity at 1550 $cm^{-1}$.

TABLE 1
Assignment of Selected Raman Peaks of R6G

| Neat R6G Experimental ($cm^{-1}$) [29] | Experimental SERS R6G our data ($cm^{-1}$) | Band assignment |
|---|---|---|
| 1184 | 1184 | In plane Xanthenes ring deformation, C-H bending, N-H bending |
| 1312 | 1311 | In plane Xanthenes ring breathing, N-H bending, $CH_2$ waggling |
| 1364 | 1362 | Xanthenes ring stretching, in plane C-H bending |
| 1512 | 1510 | Xanthenes ring stretching, C-N stretching, C-H bending, N-H bending |
| 1577 | 1575 | Xanthenes ring stretching, in plane N-H bending |
| 1651 | 1651 | Xanthenes ring stretching, in plane C-H bending |

### 3.2. SERS Performances of the Prepared Fiber Probe

It is universally acknowledged that sensitivity is essential requirement for any SERS substrate. In this paper, we use R6G as the Raman probe molecule to select the fiber probe with the strongest Raman enhancement effect among the six types of fiber probes (that is AgNPs-MMF-x, where x is 10, 20, 30, 40, 50, 60 mins, respectively).

Fig. 7(a) shows the Raman signal of R6G with a concentration of $10^{-3}$ M adsorbed on six fiber SERS probes with different assembly time. Obviously, the Raman signal intensities of six fiber SERS probes are significantly different. In addition, as shown in Fig. 7(b), we choose the prominent Raman bands at the center of 1184, 1311, 1362, 1510 and 1651 $cm^{-1}$ to quantificationally discuss the enhancement effect of six fiber SERS probes. Particularly, the Raman signals of R6G first increase with the increase of self-assembly time. When the self-assembly time is 30 mins, the Raman intensity reaches the maximum, and then decrease of Raman signal intensity could be observed by further increasing the self-assembly time. Obviously, compared with other fiber SERS probes, the AgNPs-MMF-30 probe achieves the maximum enhancement effect. For example, the Raman intensity of 1362 $cm^{-1}$ from AgNPs-MMF-30 probe is 1.70 and 1.49 times than that from AgNPs-MMF-20 probe and AgNPs-MMF-40 probe, respectively. It can be seen from Fig. 5 that when the A and B areas on the fiber surface self-assemble for 20 mins, the amount of AgNPs adsorbed is less and the dispersion is sparse. When the self-assembly time is further extended to 30 mins, the AgNPs on the inner surface of the fiber microcavity basically show a silver nano-film with full monolayer adsorption and small particle spacing. When the self-assembly time is extended to 40 mins, the surface of fiber begins to accumulate AgNPs, the nanoparticles are closely packed to form a multilayer state. There are too few or too many AgNPs, it will affect the SERS performance of the microcavity fiber SERS probe. When the self-assembly time is short, there are too few AgNPs on the surface of the fiber microcavity, and the gap between the nanoparticles is large, which directly affects its SERS enhancement effect. When the self-assembly time is too long, the AgNPs at the bottom of the microcavity will be cured too thick. The tightly packed nanoparticles will also reduce the “hot spots” in substrate [30]. The thick silver nano-layer also affects the collection of SERS signals by the fiber SERS probe. Therefore, according to the results of Fig. 7(a) and (b), we control the self-assembly time to 30 mins to prepare the fiber SERS probe.

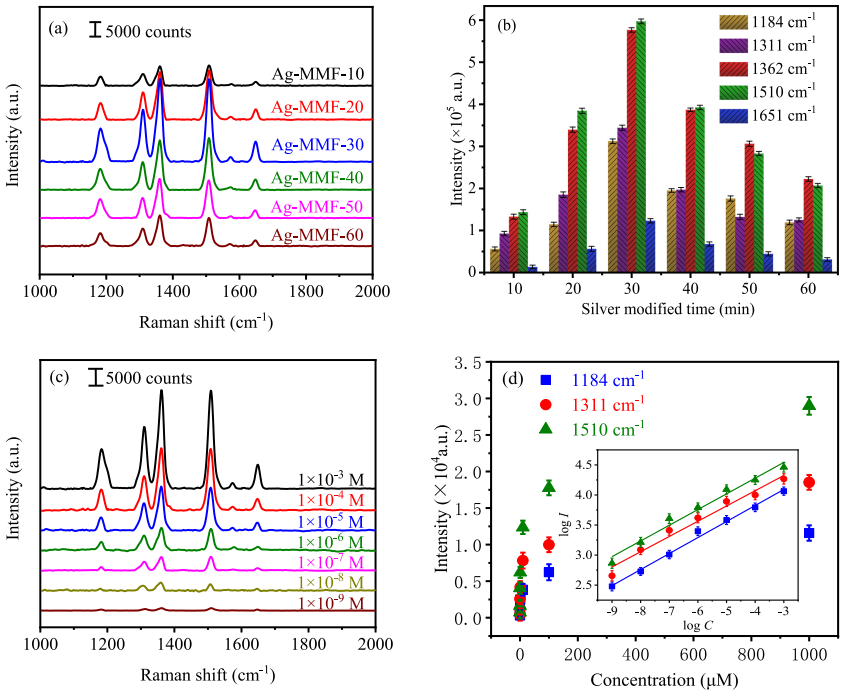


Fig. 7. Experimental results: (a) Raman spectra of $10^{-3}$ M R6G adsorbed on AgNPs-MMF probes prepared with different self-assembly time; (b) Raman intensity at 1184, 1311, 1362, 1510 and 1651 $cm^{-1}$ under different self-assembly time; (c) SERS spectra of R6G with different concentrations from $10^{-3}$ M to $10^{-9}$ M on AgNPs-MMF-30 probe; (d) the linear relationship between the log *I* of the peaks centered at 1184, 1311, 1510 $cm^{-1}$ and the log *C* of R6G (the error bars are calculated based on five independent measurements).

In order to find the LOD of the AgNPs-MMF-30 probe, SERS spectra of R6G with different concentrations are tested by the AgNPs-MMF-30 probe as shown in Fig. 7(c). Obviously, as the concentrations of the R6G decreases, the intensities of the Raman spectra decrease accordingly. When the concentration of R6G is decreased to $10^{-9}$ M, some of the R6G band peaks still can be distinguished at this ultra-low concentration. The results indicate that the AgNPs-MMF-30 probe has high sensitivity, and the LOD for adsorbed R6G molecules is $10^{-9}$ M under this experimental condition. Fig. 7(d) shows the relationship between the SERS intensity of peaks centered at 1184, 1311 and 1510 $cm^{-1}$ and the concentration of R6G. As we can see, the Raman intensity of each characteristic peak has no obvious functional relationship with the change of R6G solution. However, when Raman intensity and R6G concentration are converted to logarithmic scale at the same time, the response between log *I* and log *C* of each characteristic peak shows a good linear relationship. Meanwhile, the linear correlations between the Raman intensities of these three peaks and R6G concentrations over the range of $10^{-3}$∼$10^{-9}$ M in logarithm scale are obtained, as shown in Fig. 7(d).

Table 2 shows the relationship between log *I* and log *C* at 1184, 1311 and 1510 $cm^{-1}$. The $R^2$ of three linear fit curves in Table 2 are all greater than 0.9670 that indicated the outstanding capability for the quantitative detection of aromatic molecule. These linear relationships allow for the quantitative determination of the unknown concentrations of R6G in solutions by using the AgNPs-MMF-30 probe.

Apart from sensitivity, an outstanding fiber SERS probe should also possess key performances of reproducibility and stability which largely affect its reliability and practicability. To evaluate the reproducibility of Raman signals of our AgNPs-MMF-30 probe, 50 AgNPs-MMF-30 probes are prepared to detect R6G solution with a concentration of $10^{-4}$ M. 50 Raman spectra are obtained and 25 Raman spectra are randomly selected for analysis. As shown in Fig. 8(a), the 25 random

TABLE 2
Linear Relationships Between R6G Concentrations and Raman Intensities At Characteristic Peaks of R6G

| Peaks ($cm^{-1}$) | Linear function | Correlation coefficient ($R^2$) |
|---|---|---|
| 1184 | $y$= 0.2666$x$+ 4.8911 | 0.9915 |
| 1311 | $y$= 0.2538$x$+5.0858 | 0.9673 |
| 1510 | $y$= 0.2613$x$+ 5.3250 | 0.9760 |

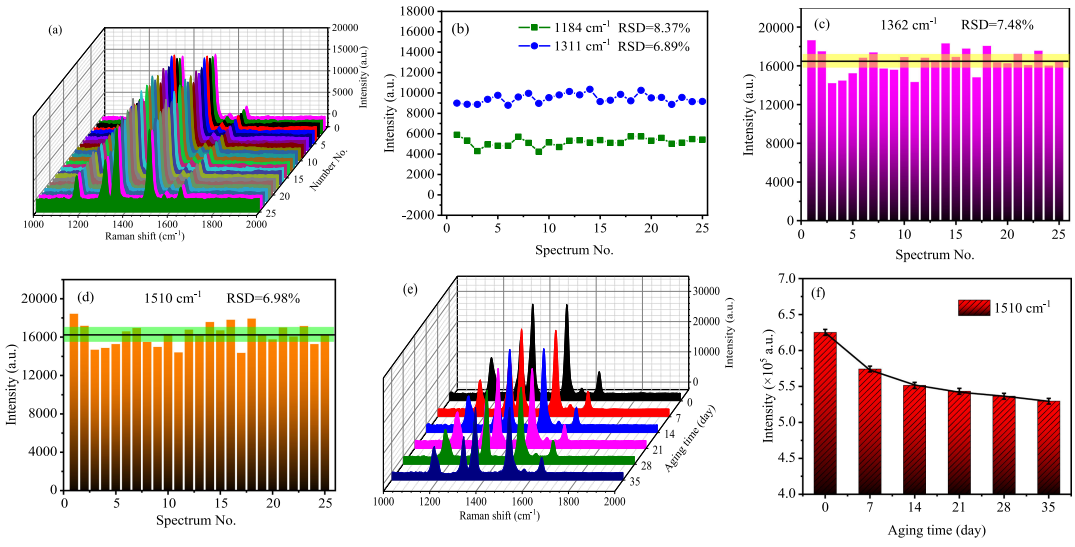


Fig. 8. Experimental results: (a) the 25 random Raman spectra of R6G with the concentration of $10^{-4}$ M; (b)∼(d) the main Raman intensities and RSD of $10^{-4}$ M R6G at characteristic Raman peaks (b:1184, 1311 $cm^{-1}$; c:1362 $cm^{-1}$; d:1510 $cm^{-1}$); (e) SERS spectra of $10^{-3}$ M R6G detected on AgNPs-MMF-30 probe with different periods; (f) plot of Raman intensities of R6G at 1510 $cm^{-1}$ versus different detection time.

Raman spectra of R6G with the concentration of $10^{-4}$ M suggest that the shapes of all the spectra match well and there is neither a shift of the position nor a change at the characteristic peaks. The result shows that the AgNPs-MMF-30 probe has good reproducibility. Generally, the RSD values of Raman intensities are calculated to assess the reproducibility of a SERS substrate. In this regard, the RSD values of 25 Raman spectra at 1184 and 1311 $cm^{-1}$ peaks shown in Fig. 8(b) are calculated according to the followed (1) [31]:

$$RSD = \sqrt{\frac{\sum_{i=1}^{n} (I_i - \bar{I})^2}{n-1}} \frac{1}{\bar{I}} \tag{1}$$

where the $n$ is the number of the Raman spectra, $I_i$ represents the Raman signal intensity of each characteristic peak and $\bar{I}$ is the average intensity of the Raman signal intensity. Meanwhile, the RSD values of other characteristic peaks at 1362 and 1510 $cm^{-1}$ are exhibited in Fig. 8(c)∼(d). The variation of RSD values for $10^{-4}$ M R6G are all within 8.37%, which further shows that the AgNPs-MMF-30 probe has good reproducibility and uniformity.

The long-term stability of Raman signals is a crucial parameter for fiber SERS probe performance and actual applications of SERS technique. 10 sets of AgNPs-MF-30 probes are prepared for later use. An AgNPs-MF-30 probe is taken out every 7 days for testing. As shown in Fig. 8(e), Raman spectra of $10^{-3}$ M R6G absorbed on AgNPs-MMF-30 probe is measured to investigate the stability. Obviously, after different aging time (0, 7, 14, 21, 28 and 35 days), the signal intensities decrease in

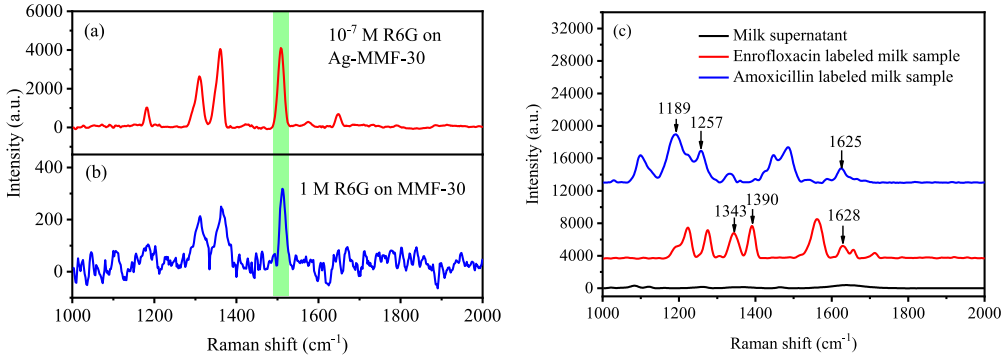


Fig. 9. Experimental results: (a)∼(b) Raman spectra of R6G measured on different substrates; (c) Raman spectra of different substances.

different degrees under the same environmental conditions. As quantitatively analyzed in Fig. 8(f), when the aging time is 7 days, the Raman intensity at 1510 $cm^{-1}$ of R6G decreases by 0.082. When the aging time is 14 days, the Raman intensity decreases by 0.118, after which the signal intensity changes relatively smoothly and tends to be stable. After 35 days of aging, the comprehensive Raman signal strength decreases by 15.3%. These results indicate that AgNPs-MMF-30 owned long-time stability. On the other hand, it can effectively reduce the waste of noble metals and fiber.

### 3.3. EF Calculation

In general, the enhancement factor (EF) value is calculated as a typical approach to evaluate the SERS enhancement performance of a fiber SERS probe. Therefore, the enhancement contribution of AgNPs-MMF-30 probe is quantified by the EF value [32] according to the following (2):

$$EF = \frac{I_{SERS}}{I_R} \times \frac{C_R}{C_{SERS}} \tag{2}$$

where the $I_{SERS}$ and $I_R$ are the SERS enhanced signal of $10^{-7}$ M R6G solution and normal Raman signal of 1 M R6G, the $C_{SERS}$ and $C_R$ are the concentration of $10^{-7}$ M R6G solution and 1 M R6G solution. Due to the normal Raman signal is measured by the microcavity fiber of unmodified AgNPs, it is difficult to detect low concentration of R6G molecules. Therefore, it is similar to the calculation method of Pham [33] that we also choose R6G with the concentration of 1M for normal Raman test. As shown in Fig. 9(a) and (b), the $I_{SERS}$ and $I_R$ of the Raman shift at 1510 $cm^{-1}$ are 4045 and 298, respectively. The EF value of AgNPs-MMF-30 probe is calculated to be $1.36 \times 10^8$. The results show that the AgNPs-MMF-30 probe has a higher SERS enhancement performance.

### 3.4 SERS Detection of Antibiotics Residues in Milk

To further demonstrate the performance of AgNPs-MMF-30 probe, the experiment for the practical application is carried out to detect antibiotics in milk. It is well known that enrofloxacin and amoxicillin are often used as a feed additive in the animal husbandry industry to play a certain role in the prevention, treatment and growth of animal diseases. If there are residues of antibiotics in the milk, long-term consumption will slowly accumulate in the human body and cause certain harm to the human body, such as a decline in human immunity, chronic human poisoning, genetic mutations and so on [3], [4]. Therefore, a rational and convenient way to detect antibiotics in milk with high sensitivity is essential. In this paper, AgNPs-MMF-30 probe is used to detect antibiotic residues in milk.

Fig. 9(c) shows the Raman spectra of the centrifuged milk supernatant, enrofloxacin spiked milk sample, and amoxicillin spiked milk sample. The Raman characteristic peak positions of enrofloxacin spiked milk samples are at 1343, 1390 and 1628 $cm^{-1}$ respectively. The Raman

TABLE 3
Assignment of Selected Raman Peaks of Enrofloxacin and Amoxicillin [34]–[36]

| Types of antibiotics | Characteristic peaks of powder ($cm^{-1}$) | Characteristic peaks of SERS ($cm^{-1}$) | Band assignment |
|---|---|---|---|
| Enrofloxacin | 1345 | 1343 | ν(C-F) |
| | 1395 | 1390 | ν(O-C-O) |
| | 1624 | 1628 | ν(C=O) |
| Amoxicillin | 1177 | 1189 | $\delta(NH_2) + \delta(CH) + \delta(OH)$ |
| | 1258 | 1257 | ν(C-OH) + δ(CH)benzene |
| | 1619 | 1625 | υ(CC ring2) + δ(N19H) |

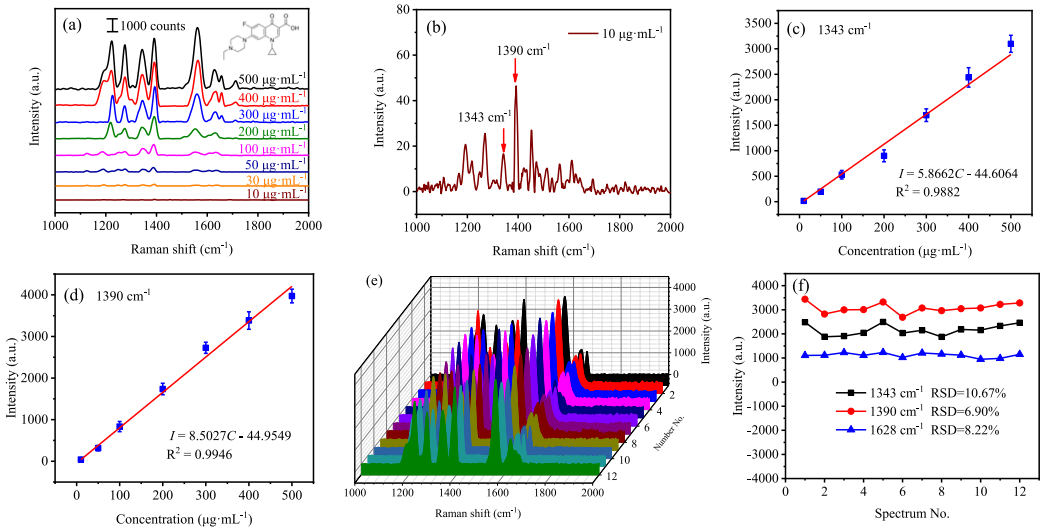


Fig. 10. Experimental results: (a) SERS spectra of enrofloxacin residues in milk with different concentrations; (b) SERS spectra of enrofloxacin residues in milk with 10 $\mu$g·mL$^{-1}$; (c)~(d) the linear relationship between the I of the peaks centered at 1343, 1390 cm$^{-1}$ and the C of enrofloxacin residues in milk(the error bars are calculated based on five independent measurements); (e) the 12 random Raman spectra of enrofloxacin with the concentration of 400 $\mu$g·mL$^{-1}$; (f) the Raman intensities and RSD of 400 $\mu$g·mL$^{-1}$ enrofloxacin at characteristic Raman peaks.

characteristic peaks of the amoxicillin spiked milk samples are at 1189, 1257 and 1625 cm$^{-1}$ respectively. The Raman spectrum of the milk supernatant has no characteristic peaks near the Raman characteristic peaks of the enrofloxacin spiked milk sample and the amoxicillin spiked milk sample. The band assignments of Enrofloxacin and Amoxicillin are listed in Table 3.

As shown in Fig. 10(a), the characteristic peaks of enrofloxacin are observed and the Raman intensities of enrofloxacin decreased with the decrease of the enrofloxacin concentrations. Fig. 10(b) shows the Raman spectrum of enrofloxacin milk sample with a concentration of 10 $\mu$g·mL$^{-1}$. It can be seen from Fig. 10(a) and (b) that the LOD for enrofloxacin in milk detected by AgNPs-MMF-30 probe is as low as 10 $\mu$g·mL$^{-1}$. Fig. 10(c) and (d) show a linear relationship between I of the integrated Raman intensities centered at 1343 and 1390 cm$^{-1}$ and C of enrofloxacin in milk concentration. Meanwhile, the $R^2$ of linear relationships are 0.9982 and 0.9946 respectively. The results show that AgNPs-MMF-30 probe can be used to quantitatively detect enrofloxacin residues in milk. Fig. 10(e) shows 12 sets of Raman spectra are randomly selected from 25 sets of SERS tests of 12 AgNPs-MMF-30 probes which have been deposited with 400 $\mu$g·mL$^{-1}$ enrofloxacin spiked milk sample. It can be seen that the shapes of all the spectra match well and there is neither a shift of the position nor a change at the characteristic peaks. Besides, Fig. 10(f) shows that the RSD values of 1343, 1390 and 1628 cm$^{-1}$ are calculated to be 10.67%, 6.90% and 8.22%, respectively. Fig. 10(e) and (f) show that AgNPs-MMF-30 has good reproducibility performance. In short, these results indicate that AgNPs-MMF-30 probe has good application value for detecting enrofloxacin residues in milk.

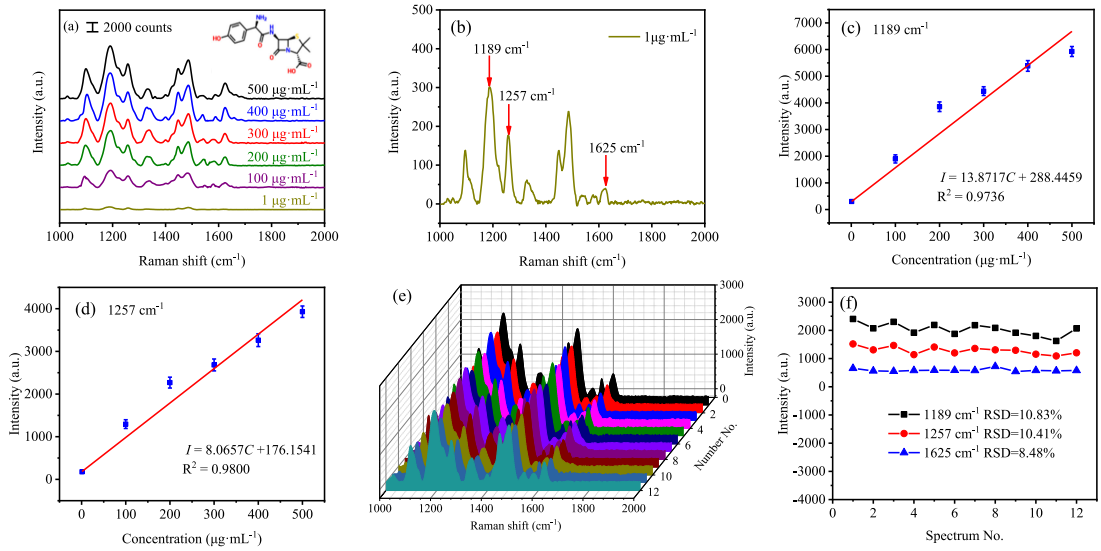


Fig. 11. Experimental results: (a) SERS spectra of amoxicillin residues in milk with different concentrations; (b) SERS spectra of amoxicillin residues in milk with 1 $\mu$g·mL$^{-1}$; (c)∼(d) the linear relationship between the I of the peaks centered at 1189, 1257 cm$^{-1}$ and the C of amoxicillin residues in milk; (e) the 12 random Raman spectra of amoxicillin with the concentration of 100 $\mu$g·mL$^{-1}$; (f) the main Raman intensities and RSD of 100 $\mu$g·mL$^{-1}$ amoxicillin at characteristic Raman peaks.

Meanwhile, the amoxicillin residue in milk is also tested. It can be seen from Fig. 11(a) that the Raman intensities of amoxicillin decreases with the decrease of amoxicillin concentrations. Fig. 11(b) shows the Raman spectrum of amoxicillin milk sample with a concentration of 1 $\mu$g·mL$^{-1}$, Raman peaks can be clearly seen at 1189, 1257 and 1625 cm$^{-1}$. It can be seen from Fig. 11 (a) and (b) that the LOD for amoxicillin in milk detected by AgNPs-MMF-30 probe is as low as 1 $\mu$g·mL$^{-1}$. Fig. 11(c) and (d) show a linear relationship between I of the integrated Raman intensities centered at 1189 and 1257cm$^{-1}$ and C of amoxicillin in milk concentration. The $R^2$ of linear relationships are 0.9736 and 0.9800 respectively. Fig. 11(e) shows the reproducibility test result of 12 sets of AgNPs-MMF-30 probes which have been deposited with 100 $\mu$g·mL$^{-1}$ amoxicillin spiked milk sample. And Fig. 11(f) shows that the RSD values of 1189, 1257 and 1625 cm$^{-1}$ are calculated to be 10.83%, 10.41% and 8.48%, respectively. The results indicate that this kind of high-performance fiber SERS probe substrate can be applied to rapidly and quantificationally detect the trace of other label-free organic molecules in real samples.

In the animal husbandry industry, a variety of antibiotic drugs are usually mixed to prevent and treat animal diseases. In order to verify the detection ability of the prepared AgNPs-MMF-30 probe for mixed antibiotics, enrofloxacin and amoxicillin are mixed to prepare mixed antibiotic spiked milk samples. AgNPs-MMF-30 probe is used to conduct SERS qualitative analysis of milk samples spiked with mixed antibiotics at a concentration of 500 $\mu$g·mL$^{-1}$. Fig. 12(b) shows the SERS signals of mixed antibiotics residue.

Through the qualitative analysis of Fig. 12(a)∼(c), it can be seen that SERS spectra of the milk samples with mixed antibiotics show the Raman characteristic peaks of enrofloxacin at 1341, 1396, 1626 cm$^{-1}$ and the Raman characteristic peaks of amoxicillin at 1194, 1255, 1626 cm$^{-1}$. Although there is a slight position offset of the characteristic peaks in the milk sample spiked, the offset is negligible within a reasonable range. Fig. 12(d) shows the reproducibility test results of AgNPs-MMF-30 probes which have been deposited with mixed antibiotic milk sample. It also can be seen that all the shape of the spectra matched well and there is neither a shift of the position nor a change at the characteristic peaks. The characteristic peaks of each antibiotic residue can be distinctively discerned in the mixed spectrum. The experimental results fully reveal that the proposed method can be used for rapid and on-spot detection of multifold antibiotics residues in

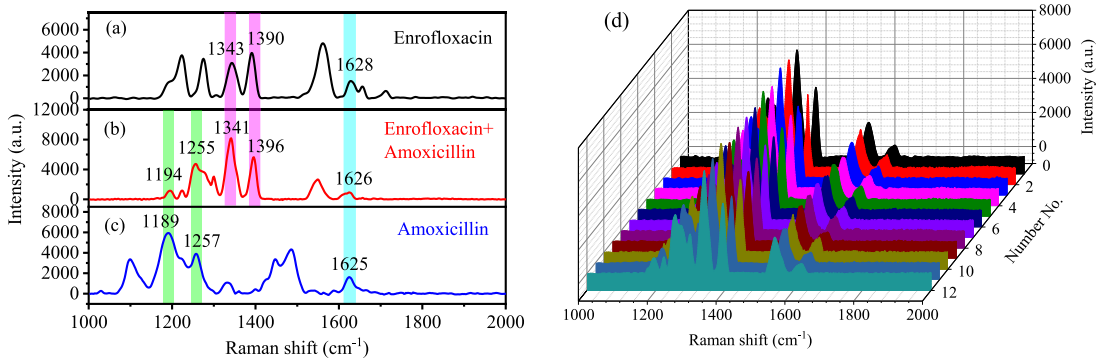


Fig. 12. Experimental results: (a) Raman spectra of enrofloxacin milk samples; (b) Raman spectra of milk samples mixed with antibiotics; (c) Raman spectra of amoxicillin milk samples; (d) the reproducibility test result of mixed antibiotic milk samples.

milk, which further proves the powerful analytical ability of the AgNPs-MMF-30 probe in practical applications.

## 4. Conclusion

In this paper, a silver-modified microcavity fiber SERS probe is successfully fabricated by sol self-assembly method. The AgNPs-MMF-x probe performance can be well controlled by adjusting the self-assembly time. The AgNPs-MMF-30 probe shows the highest enhancement efficiency for R6G molecules. The EF for AgNPs-MMF-30 probe to $10^{-7}$ M R6G is up to $1.36 \times 10^{8}$. The AgNPs-MMF-30 probe also shows a superior SERS detection sensitivity with LOD as low as $10^{-9}$ M. In addition, the RSD values for R6G are less than 10.94%, demonstrating the outstanding reproducibility of AgNPs-MMF-30 probe. The AgNPs-MMF-30 probe still shows a good stability of the Raman signal after aging for 35 days. Owing to the high performance, the trace detection of enrofloxacin and amoxicillin in milk are successfully achieved by using it. The LOD enrofloxacin and amoxicillin in milk are 10 $\mu$g·mL$^{-1}$ and 1 $\mu$g·mL$^{-1}$, respectively. Meanwhile, multicomponent antibiotic residues in milk are successfully detected. This method has certain research significance for the field test of antibiotic residues in milk. Therefore, the silver-modified microcavity fiber SERS probe can be a potential candidate in food safety and environmental monitoring.

## References

[1] D. Cheng *et al.*, "Performance of microbial fuel cell for treating swine wastewater containing sulfonamide antibiotics," *Bioresource Technol.*, vol. 311, Sep. 2020, Art. no. 123588.
[2] M. M. Bonnie and B. L. Stuart, "Food animals and antimicrobials: Impacts on human health," *Clin. Microbiol. Rev.*, vol. 24, no. 4, pp. 718–733, Oct. 2011.
[3] J. Chen, G. G. Ying, and W. J. Deng, "Antibiotic residues in food: Extraction, analysis, and human health concerns," *J. Agricultural Food Chem.*, vol. 67, no. 27, pp. 7569–7586, Jul. 2019.
[4] S. Yan, X. X. Lai, G. R. Du, and Y. Xiang, "Identification of aminoglycoside antibiotics in milk matrix with a colorimetric sensor array and pattern recognition methods," *Analytica Chimica Acta*, vol. 1043, pp. 153–160, Nov. 2018.
[5] H. Hermansson *et al.*, "Breast milk microbiota is shaped by mode of delivery and intrapartum antibiotic exposure," *Front. Nutr.*, vol. 6, pp. 1–8, Feb. 2019.
[6] I. D. Kargin, L. S. Sokolova, A. V. Pirogov, and O., and Shpigun, "HPLC determination of tetracycline antibiotics in milk with post-column derivatization and fluorescence detection," *Inorganic Mater.*, vol. 52, no. 14, pp. 1365–1369, Dec. 2016.
[7] M. Przenioso-Siwczyńska, E. Patyra, A. Grelik, M. Chyłek-Purchała, B. Kozak, and K. Kwiatek, "Contamination of animal feed with undeclared tetracyclines-confirmatory analysis by liquid chromatography-mass spectrometry after microbiological plate test," *Molecules*, vol. 25, no. 9, May 2020, Art. no. 2162.
[8] W. M. Yang *et al.*, "A stimuli response, core-shell structured and surface molecularly imprinted polymers with specific pH for rapid and selective detection of sulfamethoxazole from milk sample," *Reactive Funct. Polymers*, vol. 151, Jun. 2020, Art. no. 104578.

[9] W. J. Lian, S. Liu, L. Wang, and H. Liu, "A novel strategy to improve the sensitivity of antibiotics determination based on bioelectrocatalysis at molecularly imprinted polymer film electrodes," *Biosensors Bioelectron.*, vol. 73, pp. 214–220, Nov. 2015.
[10] O. D. Hendrickson *et al.*, "Development of a double immunochromatographic test system for simultaneous determination of lincomycin and tylosin antibiotics in foodstuffs," *Food Chem.*, vol. 318, Jul. 2020, Art. no. 126510.
[11] I. L. Wu, S. B. Turnipseed, W. C. Andersen, and M. R. Madson, "Analysis of peptide antibiotic residues in milk using liquid chromatography-high resolution mass spectrometry (LC-HRMS)," *Food Additives Contaminants: Part A*, vol. 37, no. 8, pp. 1264–1278, Jun. 2020.
[12] L. Jank, M. T. Martins, J. B. Arsand, R. B. Hoff, F. Barreto, and T. M. Pizzolato, "High-throughput method for the determination of residues of $\beta$-lactam antibiotics in bovine milk by LC-MS/MS," *Food Additives Contaminants Part A*, vol. 32, no. 12, pp. 1992–2001, Oct. 2015.
[13] I. Yariv *et al.*, "Detecting concentrations of milk components by an iterative optical technique," *J. Biophotonics*, vol. 8, no. 11/12, pp. 979–984, Feb. 2015.
[14] E. C. Le Ru and P. G. Etchegoin, "Single-molecule surface-enhanced raman spectroscopy," *Annu. Rev. Phys. Chem.*, vol. 63, no. 1, pp. 65–87, Jan. 2012.
[15] C. Andreou, R. Mirsafavi, M. Moskovits, and C. D. Meinhart, "Detection of low concentrations of ampicillin in milk," *Analyst*, vol. 140, no. 15, pp. 5003–5005, Jun. 2015.
[16] M. Muhammad, B. Yan, G. H. Yao, and K. Chao, "Surface-enhanced Raman spectroscopy for trace detection of tetracycline and dicyandiamide in milk using transparent substrate of ag nanoparticle arrays," *ACS Appl. Nano Mater.*, vol. 3, no. 7, pp. 7066–7075, Jun. 2020.
[17] M. Kosowska *et al.*, "Microscale diamond protection for a ZnO coated fiber optic sensor," *Sci. Rep.*, vol. 10, no. 1, Nov. 2020, Art. no. 19141.
[18] T. Hutter, S. R. Elliott, and S. Mahajan, "Optical fibre-tip probes for SERS: Numerical study for design considerations," *Opt. Exp.*, vol. 26, no. 12, pp. 15539–15550, Jun. 2018.
[19] Y. Liu *et al.*, "Highly sensitive fibre surface-enhanced raman scattering probes fabricated using laser-induced self-assembly in a meniscus," *Nanoscale Cambridge*, vol. 8, no. 20, pp. 10607–10614, Jan. 2016.
[20] Y. Liu *et al.*, "Micro-coffee-ring-patterned fiber SERS probes and their in situ detection application in complex liquid environments," *Sensors Actuators B: Chem.*, vol. 299, Aug. 2019, Art. no. 126990.
[21] Y. Geng, Z. Yin, X. Tan, Y. Du, X. Hong, and X. Li, "Femtosecond laser ablated pyramidal fiber taper-SERS probe with laser-induced silver nanostructures," *IEEE Photon. J. Phys. D: Appl. Phys.*, vol. 51, no. 28, Jun. 2018, Art. no. 285104.
[22] V. Tran, B. Walkenfort, M. König, M. Salehi, and S. Schlücker, "Rapid, quantitative, and ultrasensitive point-of-care testing: A portable sers reader for lateral flow assays in clinical chemistry," *Angewandte Chemie Int. Ed.*, vol. 58, no. 2, pp. 442–446, Jan. 2019.
[23] J. Zhu, M. J. Liu, J. J. Li, X. Li, and J. W. Zhao, "Multi-branched gold nanostars with fractal structure for SERS detection of the pesticide thiram," *Spectrochimica Acta Part A*, vol. 189, pp. 589–593, Jan. 2018.
[24] J. H. Dai *et al.*, "Fiber-optic Raman spectrum sensor for fast diagnosis of esophageal cancer," *Photon. Sensors*, vol. 9, no. 1, pp. 53–59, Mar. 2019.
[25] Z. Yin *et al.*, "Sensitivity-enhanced U-shaped fiber SERS probe with photoreduced silver nanoparticles," *IEEE Photon. J.*, vol. 8, no. 3. Jun. 2016, Art. no. 6803607.
[26] Z. Y. Chen *et al.*, "Gold nanoparticles-modified tapered fiber nanoprobe for remote sers detection," *IEEE Photon. Technol. Lett.*, vol. 26, no. 8, pp. 777–780, Apr. 2014.
[27] E. J. Smythe, M. D. Dickey, J. Bao, G. M. Whitesides, and F. Capasso, "Optical antenna arrays on a fiber facet for in situ surface-enhanced Raman scattering detection," *Nano Lett.*, vol. 9, no. 3, pp. 1132–1138, Mar. 2009.
[28] L. Jensen and G. C. Schatz, "Resonance Raman scattering of rhodamine 6G as calculated using time-dependent density functional theory," *J. Phys. Chem. A*, vol. 110, no. 18, pp. 5973–5977, May. 2006.
[29] S. L. Smitha, K. G. Gopichandran, T. R. Ravindran, and V. S. Prasad, "Gold nanorods with finely tunable longitudinal surface plasmon resonance as SERS substrates," *Nanotechnology*, vol. 22, no. 26, May. 2011, Art. no. 265705.
[30] A. Foti, C. D.´ Andrea, F. Bonaccorso, and M. Lanza, "A shape-engineered surface-enhanced Raman scattering optical fiber sensor working from the visible to the near-infrared," *Plasmonics*, vol. 8, no. 1, pp. 13–23, Mar. 2013.
[31] M. Parsons, D. R. Ekman, T. W. Collette, and M. Viant, "Spectral relative standard deviation: A practical benchmark in metabolomics," *Anal.*, vol. 134, no. 3, pp. 478–485, Mar. 2009.
[32] M. Celik, S. Altuntas, and F. Buyukserin, "Fabrication of nanocrater-decorated anodic aluminum oxide membranes as substrates for reproducibly enhanced SERS signals," *Sensors Actuators B: Chem.*, vol. 255, pp. 2871–2877, Feb. 2018.
[33] B. T. Pham *et al.*, "Detection of permethrin pesticide using silver nano-dendrites SERS on optical fibre fabricated by laser-assisted photochemical method," *Sci. Rep.*, vol. 9, no. 1, pp. 238–242, Aug. 2019.
[34] M. L. He, M. S. Lin, H. Li, and N.-J. Kim, "Surface-enhanced raman spectroscopy coupled with dendritic silver nanosubstrate for detection of restricted antibiotics," *J. Raman Spectrosc.*, vol. 41, no. 7, pp. 739–744, Jul. 2010.
[35] Y. J. Peng, M. H. Liu, X. F. Chen, H. C. Yuan, and J. H. Zhao, "Surface-enhanced raman spectroscopy coupled with gold nanoparticles for rapid detection of amoxicillin residues in duck meat," *Spectrosc. Lett.*, vol. 50, no. 10, pp. 579–584, Nov. 2017.
[36] W. Ji, W. Wang, H. Qian, and W. Yao, "Quantitative analysis of amoxicillin residues in foods by surface-enhanced raman spectroscopy," *Spectrosc. Lett.*, vol. 47, no. 6, pp. 451–457, Apr. 2014.